COMPUTATIONAL CONNECTIONISM WITHIN NEURONS: A MODEL OF CYTOSKELETAL AUTOMATA SUBSERVING NEURAL NETWORKS

Steen RASMUSSEN[a,1], Hasnain KARAMPURWALA[b], Rajesh VAIDYANATH[b], Klaus S. JENSEN[c] and Stuart HAMEROFF[d,1]

[a]*Center for Nonlinear Studies and Theoretical Division (T-13), MS-B258, Los Alamos National Laboratory, Los Alamos, NM 87545, USA*

[b]*Department of Electrical and Computer Engineering, University of Arizona, USA*

[c]*Department of Anesthesiology, University of Colorado, USA*

[d]*Advanced Biotechnology Laboratory, Department of Anesthesiology, University of Arizona College of Medicine, Tucson, AZ 85724, USA*

"Neural network" models of brain function assume neurons and their synaptic connections to be the fundamental units of information processing, somewhat like switches within computers. However, neurons and synapses are extremely complex and resemble entire computers rather than switches. The interiors of the neurons (and other eucaryotic cells) are now known to contain highly ordered parallel networks of filamentous protein polymers collectively termed the cytoskeleton. Originally assumed to provide merely structural "bone-like" support, cytoskeletal structures such as microtubules are now recognized to organize cell interiors dynamically. The cytoskeleton is the internal communication network for the eucaryotic cell, both by means of simple transport and by means of coordinating extremely complicated events like cell division, growth and differentiation. The cytoskeleton may therefore be viewed as the cell's "nervous system". Consequently the neuronal cytoskeleton may be involved in molecular level information processing which subserves higher, collective neuronal functions ultimately relating to cognition. Numerous models of information processing within the cytoskeleton (in particular, microtubules) have been proposed. We have utilized cellular automata as a means to model and demonstrate the potential for information processing in cytoskeletal microtubules. In this paper, we extend previous work and simulate associative learning in a cytoskeletal network as well as assembly and disassembly of microtubules. We also discuss possible relevance and implications of cytoskeletal information processing to cognition.

1. Cognition: emergent computation in the brain

1.1. Connectionism

The use of connectionist models of functional brain organization has advanced understanding of cognition and linked neuroscience to computer science. "Neural networks", which approximate cortical neurons as parallel processors with variable lateral interconnections, may be simulated on computers and can provide a working model of some aspects of brain function [32, 41]. A key concept relating neural network dynamics to neuroscience was introduced by Hebb [40]. He hypothesized that spatially organized neural networks called "cell assemblies" function as reverberatory circuits which constituted elements of thought. Gazzaniga's [30] "modules", Minsky's [55] "agents", Freeman's [26] "cartels" and other conceptualized functional entities are examples of more recent, comparable proposals for anatomic neural networks. In Hebb's view, an individual neuron could participate in many cell assemblies just as an individual member of society may participate in many social groups. By strengthening or reinforcing repeatedly used connections ("synaptic plasticity"), Hebb suggested that recognition, learning and problem solving occurred

[1]To whom all correspondence should be sent.

0167-2789/90/$03.50

through lowered thresholds of specific loops. By assigning energy levels to threshold loop patterns ("landscapes"), mathematical solutions could be applied to neural net configurations [41].

There are, however, at least two inconsistencies in the analogy between neural nets and brain function. The first is that neurons and their synapses are extremely complex and by themselves resemble computers more than fundamental switches. Accordingly, further attempts to approach mechanisms of brain cognition need to consider dynamic regulatory activities within each neuron. The second is that a number of important artificial neural networks require "back propagation": tuning of internal parameters from output conditions. Both of these inconsistencies may be resolved by consideration of the cytoskeleton, an intracellular parallel network of protein polymers which regulate synapses and performs other important functions.

We contend that rudimentary information processing occurs within and among intraneuronal cytoskeletal elements such as microtubules (MTs) (fig. 1). By subserving synaptic connectionism, such information processing can provide a lower level in a hierarchy of cognitive processes from whose highest level emerges consciousness. Further, retrograde patterns travelling through the cytoskeleton could serve a role analogous to back-propagation in some artificial neural networks. In sections 4 and 5, we describe simulation of such retrograde patterns travelling through microtubules.

In the cytoskeleton, filamentous bridges among parallel MTs and/or neurofilaments could serve functions comparable to the recognition automata of Reeke and Edelman [61]. To take maximal advantage of parallelism, these authors have modelled two parallel automata which communicate laterally and have distinct and complementary personalities. One model automaton ("Darwin") is highly analytical, keyed to recognizing edges, dimensions, orientation, color, intensity, etc. The other ("Wallace") is more "gestalt" and attempts to merely categorize objects into preconceived

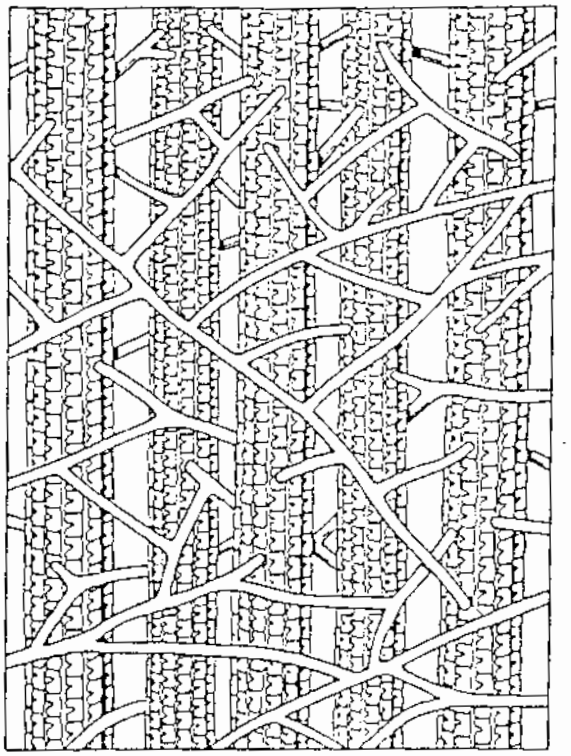

Fig. 1. Connectionist network of five parallel arrayed microtubules (MTs) interconnected by lateral crosslink filaments. Drawn by Fred Anderson from electron micrograph of neuronal dendrite cytoplasm (Aoki and Siekevitz [5]).

classifications. Lateral communications between the two parallel automata resolve conflicting output and form an associative memory. In the cytoskeleton, filamentous bridges among parallel MTs and/or neurofilaments could serve comparable functions.

Multi-level nets are consistent with connectionist brain models in which neural net "assemblies", "modules", etc. fit in an overall cognitive hierarchy of parallel layers of brain/mind organization [13, 20]. The highest cognitive level in such models is global brain function which correlates with awareness, thought, or "consciousness" (although some would argue for even higher-level social consciousness among people, political parties, societies, etc. [42, 59]). The second level appears to be comprised of anatomically and functionally recognizable brain systems and centers (i.e. respiratory

center, satiety center, etc. [66]). At intermediate levels, maps such as the motor and sensory homunculi represent the body and outside world. Finally, the lowest level is thought to be the neural synaptic network, module or cartel which may operate cooperatively by utilizing dense interconnectedness, parallelism, associative memory and learning due to synaptic plasticity.

The lowest level of brain/mind organizational hierarchy, and potential correlate of the binary switch in computers, is generally considered to be the neuronal synapse. However, we suggest that information processing in the cytoskeleton could provide a basement level to the cognitive hierarchy. The cytoskeleton is a parallel, interconnected network of microtubules, actin, and intermediate filaments which also connects to membrane proteins, cell nuclei, centrioles and other structures. Capabilities for dynamic organization coupled with the cytoskeleton's grid-like lattice structure have prompted at least a dozen author groups to model microtubules and other cytoskeletal structures as information processing devices [35]. In neurons, synaptic connectionism and regulation (plasticity) depend on cytoskeletal functions as do other cognitive processes. Information representation, transduction, translocation (including retrograde signaling suitable for "back-propagation") and computation in the cytoskeleton may function just below synaptic neural networks in a cognitive hierarchy.

The next sections will describe: (1.2) evidence linking the cytoskeleton to computation, (2) a biochemical overview of microtubules and other cytoskeletal elements, and (3) models of cytoskeletal information processing. In section 3.3, our previously published model of molecular automata in microtubules [39] is reviewed. Section 4 describes a network model of connected microtubule automata capable of learning and association and section 5 covers an assembly/disassembly microtubule automata model relevant to cell division, growth and plasticity. Section 6 concludes with a discussion of the potential implications of cytoskeletal computation.

1.2. Cytoskeleton and computation

The concept of cytoskeletal computation is based on the observation that cytoplasmic interiors of living cells, particularly nerve cells, are not watery soups. The current picture of cell interiors is one of a highly organized network in which cell water is bound and governed by cytoskeletal structures rather than a freely diffusing solution of macromolecules. Two lines of evidence support this concept. The first is the cytoskeleton which interpenetrates the cytoplasm and defines its architecture and function. Some cytoskeletal components are in polymerization equilibrium, interconverting cytoplasm between "sol" (liquid, solution) and "gel" (gelatinous, viscous) states. This "sol/gel" equilibrium (mediated by Ca^{2+} and Mg^{2+} effects on cytoskeletal actin and other proteins) indicate that the interiors of living cells operate very close to the solid–liquid phase transition. Theoretical findings predict optimal computational capabilities for distributed dynamical systems near this phase transition [47, 58].

Another line of evidence supporting the possibility of a computational cytoplasm includes data from nuclear magnetic resonance (NMR), neutron diffraction and other techniques which show a high degree of bound water in the cytoplasm. Water molecules abutting cytoskeletal (and other) cytoplasmic surfaces are attracted to these surfaces and are restricted in their motions. As a result, a greater proportion has four (rather than three or less) hydrogen bonds with their neighbors. Such water is called "vicinal" water, and has unusual properties compared to "bulk" water: lower density, greater heat capacity and greater viscosity. Further, such vicinal water may cooperatively oscillate with coherent excitations in cytoskeletal proteins (section 3.2).

Further circumstantial evidence for cytoskeletal computation and communication stems from the spatial distribution of discrete sites/states in the cytoskeleton. For example, subunits in microtubules have a "density" of about 10^{17} per cm^3, very close to the theoretical limit for charge sepa-

ration [34]. Thus, cytoskeletal arrays have maximal density for information storage via charge, and the capacity for dynamically coupling that information to mechanical and chemical events via conformational states of proteins (i.e. Fröhlich's mechanism of dipole excitations coupled to conformational state).

The dynamic complexity of neurons and their synaptic connections suggest that they utilize "lower" layers which may include dendritic processing, branch point conductance and molecular dynamics [14, 63]. Lynch and Baudry [51] have studied long-term potentiation ("LTP") of synaptic efficacy in glutamate–NMDA hippocampal neurons, a correlative model of learning. They find that LTP depends on rearrangement of subsynaptic cytoskeleton – a dynamic network of parallel arrayed, interconnected proteins including microtubules, actin, and intermediate filaments. Desmond and Levy [21] have studied dendritic spine structural changes during a synaptic learning paradigm. They find mechanical shape changes in spines mediated by cytoskeletal actin connected to microtubules in dendrites. Aoki and Siekevitz [5] have studied dendritic spine synaptic plasticity in development and find that synaptic down-regulation occurs in conjunction with depolymerization of microtubules in the main dendrite. They find also that signaling and regulation for dendritic spine synapse function depends on phosphorylation of a cytoskeletal protein: MAP2. Microtubule associated proteins (MAPs) attach to and connect microtubules to other microtubules, actin, intermediate filaments, organelles, membrane proteins and cell nucleus. MAP2 is found only in neuronal dendrites, and consumes a large proportion of phosphorylation energy. MAP2 phosphorylation is regulated by cyclic AMP-dependent protein kinase and calcium–calmodulin protein kinase. Theurkauf and Vallee [68] have found MAP2 to be "the major substrate for endogenous cyclic AMP-dependent phosphorylation in cytosolic brain tissue", and concluded that MAP2 phosphorylation "may be an important reaction in response to neurotransmitter stimulation". Thus, numerous mechanisms exist for coupling membrane synaptic events and cytoskeletal activities.

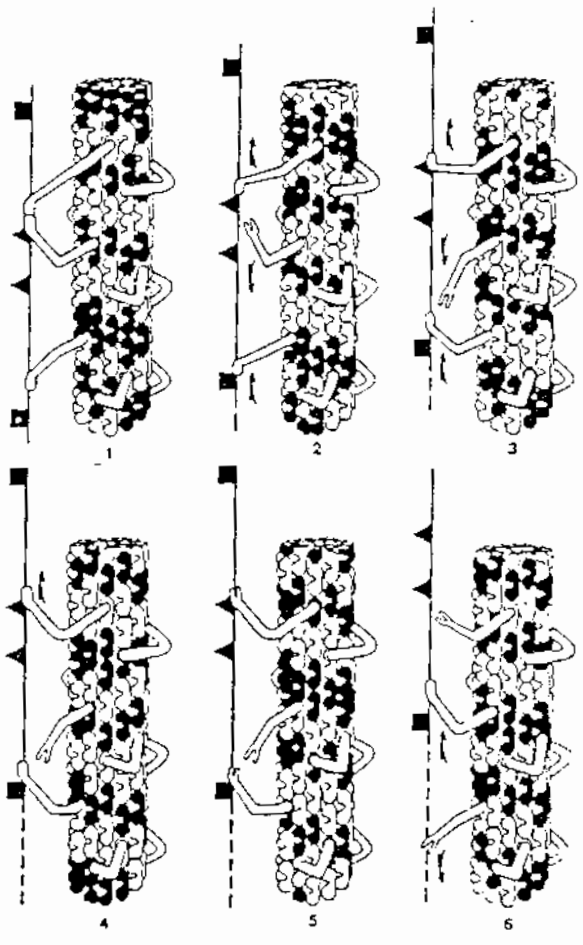

Fig. 2. Axoplasmic transport by coordinated activities of microtubule attached contratile (MAP) proteins ("dynein"). The orchestration mechanism is unknown, but shown here as the consequence of traveling conformational patterns on the MTs. By Fred Anderson.

Maintenance and modulation of synaptic function also depend on axoplasmic transport, an MT based conveyor system which supplies structural components to synapses [48, 57]. Contractile "sidearm" MAPs attached at specific sites on microtubules pass materials in a cooperative bucket brigade which achieves a velocity of 400 mm/day (fig. 2). The contractile sidearms hydrolyze ATP for energy, but the mechanism of orchestration and signaling is unknown. Material can travel in

opposite directions along a single microtubule. Other organized activities in cytoskeletal structures help control the molecular machinery of cell division, growth, differentiation, formation of synapses and dendritic spines, as well as relatively complex functions within single cell organisms like amoeba and paramecium which occur without benefit of brain, neuron, or synapse [22, 65].

Evidence for direct cytoskeletal involvement in cognitive processes comes from Mileusnic et al. [54], who have correlated production of MT subunit protein ("tubulin") and microtubule activities with peak learning, memory and experience in baby chick brain. Cronly-Dillon and co-workers [16] have shown that when baby rats first open their eyes, neurons in visual cortex begin producing vast quantities of tubulin. When the rats are 35 days old and the critical learning phase is over, tubulin production is drastically reduced. Other studies have shown that cytoskeletal proteins directly link to nerve membrane ion channels and receptors [46, 70] and that the intra-neuronal cytoskeleton is linked to nerve membrane excitability and synaptic transmission [2, 53]. Direct evidence for signal propagation in MT has been generated by Vassilev et al. [71], who suspended parallel excitable membranes in ionic solution. Only when two membranes were connected by MTs, excitation in one membrane provoked excitation in the other. The authors suggested that similar communication signals occurred routinely within the cytoskeleton. Also, Becker et al. [10] studied energy resonance transfer among fluorescent groups separately attached to different MT subunits or to membranes. They showed energy resonance transfer occurs both among MT subunits and among MT subunits and membrane proteins.

The intra-neuronal, sub-synaptic cytoskeleton is important to neural function including synaptic plasticity. In assessing cognition, low-level processing may be important. Because the cytoskeleton comprises a connectionist network within each branching neuron, it may be described as a cytoskeletal forest within each dendritic tree.

2. Microtubules and the cytoskeleton

2.1. Cytoplasm

Neurons and other cells are comprised of protoplasm, which in turn consists of membranes, organelles, nuclei, and the bulk interior medium of living cells: cytoplasm. Nineteenth century light microscopists described cytoplasm as containing or consisting of "reticular threads", "alveolar foam", or "watery soup". Development of the electron microscope through the 1960's did not initially illuminate the substructure of cytoplasm because the commonly used fixative (osmium tetroxide) was dissolving fine structure and the cell was still often perceived to be a "bag of watery enzymes".

In the early 1970's, with the event of glutaraldehyde fixation, delicate tubular filamentous structures were found in virtually all cell types and they came to be called microtubules. Originally thought to provide merely structural, or bone-like support, MTs and other filamentous structures such as actin, intermediate filaments and centrioles were collectively termed the "cytoskeleton". Recognition that complex dynamic activities of microtubules and other cytoskeletal elements were essential for organization, movement and growth of cellular cytoplasm finally brought the cytoskeleton out of the closet.

2.2. Cytoskeletal networks

Bulk cytoplasm contains networks of individual microtubules, arrayed in parallel and interconnected by filamentous strands. Other interconnecting networks of smaller filamentous proteins (actin, intermediate filaments, microtrabecular lattice, etc.) intersperse with MTs to form a dynamic gel whose activities in all types of cells (i.e. mitosis, growth and differentation, locomotion, food ingestion or phagocytosis, synapse modulation, dendritic spine formation, cytoplasmic movement, neurotransmitter release, etc.) are essential to the living state [18]. Orientation and directional guid-

ance of these cytoskeletal functions depend on centrioles: assemblies of nine pairs or triplets of microtubules arranged in replicating super-cylinders always found in pairs oriented perpendicular to each other. To initiate cell mitosis, centriole pairs migrate to opposite poles of the cell from where MT "mitotic spindles" separate chromosomes and establish orientation and architecture for the next generation cells [17, 19].

2.3. *Microtubules*

Of the various filamentous structures which comprise the cytoskeleton, microtubules are the most prominent, best characterized and appear best suited for dynamic information processing [22, 65].

MT are hollow cylinders 25 nm in diameter whose lengths may span meters in some mammalian neurons. MT cylinder walls are assemblies of 13 longitudinal protofilaments which are each a series of subunit proteins known as tubulin (fig. 3). Each tubulin subunit is a polar, 8 nm dimer which consists of two slightly different classes of 4 nm, 55 kilodalton monomers known as α and β tubulin. Genes for α and β tubulin are complex, multi-gene families which give rise to varying tubulin isozymes. During evolution some tubulins have been highly conserved for basic cell functions. However, extensive microtubule heterogeneity exists in complex cells due to genetic diversity, expression, post-translational modifications, MAPs, and assembly patterns [24, 31]. For example, two-dimensional gel electrophoresis has shown 17 different β tubulin isozymes exist in mammalian brain MTs, whereas fewer exist in other tissues [49].

The tubulin dimer subunits within MTs are arranged in a hexagonal lattice which is slightly twisted, resulting in differing neighbor relationships among each subunit and its six nearest neighbors (fig. 4).

MT self-assembly and disassembly are dynamic, complex processes which depend on various factors including temperature and calcium ion concentration. Oriented by centrioles, MT polymerization determines the architecture and form of cells which can quickly change by MT depolymerization and reassembly in another direction [45]. GTP, an energy-providing analog of ATP, binds to polymerizing tubulin; GTP hydrolysis energy is subsequently delivered to assembled MTs. MTs whose ends are GTP tubulin are stable and will continue to grow. After the GTP is hydrolyzed to GDP, GDP tubulin is exposed at MT ends and unless stabilized by MAPs, centrioles or other structures, MTs rapidly disassemble with their component subunits being utilized by assembling MTs. This dynamic instability results in a "selectionist" activity in which MT networks can probe or retreat in cellular appendages including dendritic synapses. The precise mechanism of consumption of GTP hydrolysis energy in MTs is not understood, although one possible utilization is the production of solitons or coherent lattice excitations as proposed by Fröhlich [27–29]. It is known that GTP tubulin and GDP tubulin have different conformational states [8].

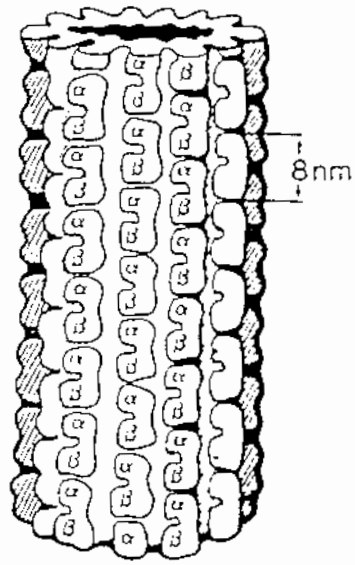

Fig. 3. Microtubules (MTs) are cylinders whose walls are 13 protofilaments, each a string of 8 nm tubulin dimers. Alpha and beta tubulin monomers form the dimers: each dimer has 6 neighbors. Drawn by Fred Anderson from X-ray crystallographic data of Amos and Klug [4].

When viewed in cross section by electron microscopy, MT outer surfaces are surrounded by a "clear zone" of several nm, which apparently represents an electronegative field due to excess electrons in tubulin and may also serve to organize cytoplasmic water and enzymes [67]. MTs, as well as their individual dimers, have dipoles with negative charges localized toward α monomers [17]. Thus MTs are "electrets": oriented assemblies of dipoles which are predicted to have piezoelectric properties [7, 52]. Contractile or enzymatic MAP proteins may be attached to MTs at specific dimer sites and MAP attachments can result in various helical patterns on MT surface lattices [12]. Contractile MAPs participate in axoplasmic transport while other MAPs form bridges which laterally connect specific subunits on parallel arrayed MTs.

3. Models of microtubular information processing

3.1. Cytoskeletal signal processing

The lattice polymer structure of MTs have suggested capabilities for information processing, and numerous author groups (some of which are mentioned below) have published theoretical models of MT/cytoskeletal information processing.

Atema [6] proposed that cellular sensory transduction occurred by propagated conformational changes in MT subunits. His view was an "all or none" propagation in which entire MTs were essentially trigger switches.

Barnett [9] proposed that filamentous cytoskeletal structures operated like information strings analogous to word processors. He proposed that MTs are processing channels along which strings of information can move, and that neurofilaments (intermediate filaments within neurons) are parallel arrayed memory channels. While not specifying the mechanism of pattern representation within MTs or neurofilaments, Barnett's model emphasizes the potential utility of parallel arrays of laterally interconnected molecular structures.

A model which does address patterns within MTs was proposed by Roth and Pihlaja [62]. They suggested conformational states of tubulin subunits within MTs were regulated by binding of inter-MT linkages of MAPs. They assumed five possible conformational states for each tubulin subunit (based on drug binding studies) could be induced by proximity of MAP binding and cooperative allosteric effects.

Hameroff and Watt [36] proposed that conformational states of tubulin within MTs were coupled to charge or dipole states, and interacted cooperatively with neighbor tubulin states. Such interactions were thought to be based on "molecular automata" in which the conformational states of individual tubulin dimer subunits represent "bits" of information subject to dynamic influence by neighboring subunits [36–39, 64]. The control of protein conformation is, by itself, an interesting enigma. Before considering molecular automata as a specific model of MT information processing, some aspects of protein conformational regulation theory will be mentioned.

3.2. Coherent protein dipole excitations

Proteins are vibrant, dynamic structures in physiological conditions. A variety of recent techniques have shown that proteins and their component parts undergo conformational motions over a range of time scales from 10^{-15} s to many minutes with the functionally most significant conformational vibrations appearing in the "nanosecond" range of 10^{-9}–10^{-11} s. Biologically relevant motions of globular proteins in this time scale are thought to include collective elastic modes, e.g. solitons and other nonlinear motions, and coherent excitations [43, 44, 60]. These motions are global changes in protein conformation rather than more rapid thermal fluctuations of side chains or local regions. Such global protein conformations appear suitable for computation: finite states which can be influenced by dynamic neighbor interactions.

Collective conformational states near the nanosecond time domain have been woven into a theory of coherent protein excitations by Fröhlich [27–29]. Changes in protein conformation, according to Fröhlich [28], are triggered by charge redistributions such as dipole oscillations within specific hydrophobic regions of proteins. Another concept of Fröhlich [27] is that a set of proteins connected in a common physical structure and electromagnetic field such as within a polarized membrane (or polymer electret like a microtubule) may be excited coherently if chemical energy such as ATP or GTP were supplied. Coherent excitation frequencies of the order of 10^9–10^{11} Hz are deduced by Fröhlich, who cites as evidence sharp windows of sensitivity to electromagnetic energy in this region by a variety of biological systems [33]. Circumstantial evidence for Fröhlich's activities in microtubules include the apparent electronegative field surrounding MTs, and the unexplained consumption of GTP hydrolysis energy by MT lattices. Other aspects of Fröhlich's model include metastable states (longer-lived conformational state patterns stabilized by local factors) and polarization waves, i.e. travelling regions of conformational states slightly out of phase with the majority of coherently excited states.

3.3. *Molecular automata in microtubules*

Conrad and coworkers [15] introduced the idea of "molecular" automata within neurons as a basis for intracellular information processing related to cognition. We believe molecular automata activities in cytoskeletal structures such as microtubules could explain much of their organizational activities.

Automaton behavior including dynamic patterns and capabilities for computation require a lattice whose subunits can exist in two or more states at discrete time steps, and transition rules which determine those states among lattice neighbor subunits. Fröhlich's [27] model of coherent excitations and cooperative coupling among proteins arrayed in an electromagnetic field may be applied to tubulin subunit dimers within MTs to serve as a "clocking" mechanism and define discrete generations for automaton behavior. We can obtain an estimate for the clocking frequency assuming one coherent "sound" wave across the MT diameter ($\Phi \simeq 25$ nm). A crude calculation, assuming that $V_{sound} \simeq 10^3$ m/s, yields a clocking frequency of approximately 4×10^{11} Hz for one wave across the MT diameter. This is in the predicted range and correlates with a clocking generation time of 2.5×10^{-11} s. However, faster and slower automata are possible, depending on the type of MT excitation being considered.

Orientation or phase of any tubulin subunit dimer relative to the coherently oscillating majority at any excitation period would depend on factors such as initial conformational states, binding of water, ions, or MAPs, bridges to other MTs, tyrosinated/glutamated state, energy-providing phosphate nucleotides (i.e. GTP) and associated proteins, genetically determined subunit factors and electrostatic dipole interactions among neighboring subunits. Many of these factors may be considered programming modes (either hereditary or environmental) whose net effects would serve to alter phases of particular subunits in coherently excited arrays. To simulate MT molecular automata, we will focus solely on electrostatic dipole interactions among MT subunits.

Our derivation of automaton neighborhoods and neighbor dynamics for computer simulation are illustrated in figs. 4 and 5. The MT cylinder (25 nm in diameter) has a circumference of 13 tubulin subunit dimers and the pitch pattern (angle from horizontal) of the leftward helix is one and one-half dimers. For automaton simulation we consider seven-member neighborhoods of tubulin dimers: a central dimer surrounded by a tilted hexagon of six neighbor dimers. Taking the cylinder axis of the MTs to define the y-axis, the dimer neighborhood is defined as follows (fig. 4): "C" is the center dimer and "N" (north) is the nearest-neighbor dimer in the positive direction of the y-axis. Similarly, dimers labeled "NE" (northeast), "SE" (southeast), "S" (south), "SW" (southwest),

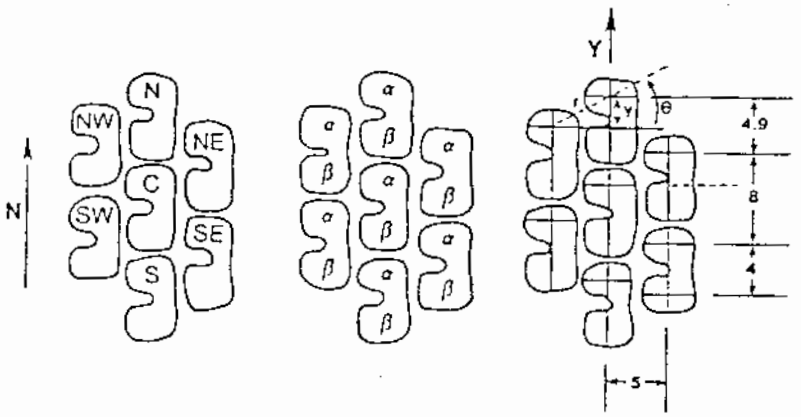

Fig. 4. Microtubule automata (MTA) neighborhood. Left: Definition of neighborhood dimers. Center: α and β monomers within each dimer are labelled. Right: Distances (in nm) and orientation among lattice neighbors. Interaction forces are calculated using $y_i = r_i \sin\theta$.

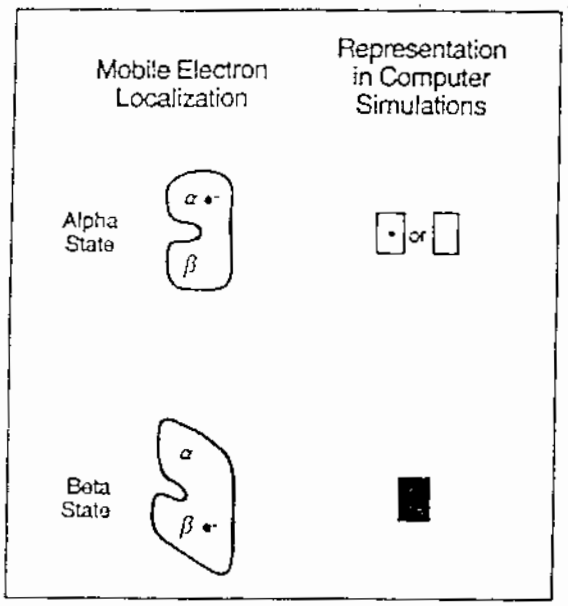

Fig. 5. Switching between conformational states in microtubule (MT) dimers. Top row: α states, bottom row: β states. Left: dimer conformation coupled to mobile electron localization. Right: representation of states in computer simulation.

and "NW" (northwest) are appropriately oriented around the "C" dimer. Within each dimer the α monomer is north of its β partner. The helical twist yielding an offset along the y-axis for NW, SW, NE, and SE neighbors leads to neighbor dimer distances and dipole interaction forces which differ among the six neighbors surrounding the C dimer.

To calculate the neighbor dipole interaction forces as a basis for automaton transition rules, each dimer may be viewed as having a mobile electron shared by the two monomers (fig. 5). At each time step the electron's average position is considered to be oriented either more toward the α monomer ("alpha state") or more toward the β monomer ("beta state") with associated changes in dimer conformation. Experimental evidence [69] suggests that a conformational shift of 29° from vertical may occur. Because MT net dipoles are negative toward the α ends, oscillations need not necessarily change direction totally to effect a conformational change. For example, a relative dipole reorientation toward the α monomer may be sufficient to induce a tubulin dimer conformational state. For our calculations, however, we have assumed that electrons localize in the centers of the two monomers.

Considering the MT lattice geometry, the y-component of the resulting electrostatic force acting on an electron in a central dimer can then be calculated as:

$$f_{\text{net}} = \frac{e^2}{4\pi\epsilon} \sum_{i=1}^{6} \frac{y_i}{r_i^3}, \qquad (1)$$

Table 1
Relative forces ($= -1000y/r^3$) for neighbor configurations. Net forces are summation of six neighbors.

Neighbor position	Central dimer α		Central dimer β	
	neighbor α	neighbor β	neighbor α	neighbor β
north	+15.625	+62.500	+6.944	+15.625
northeast	+15.205	−7.022	+9.635	+15.205
southeast	−14.250	−8.338	−7.022	−14.250
south	−15.625	−6.944	−62.500	−15.625
southwest	−15.205	−9.635	+7.022	−15.205
northwest	+14.250	+7.022	+8.338	+14.250

where y_i and r_i are defined as illustrated in fig. 4, e is the electron charge, and ϵ is the average permittivity for MT proteins, typically 10 times the vacuum permittivity [50]. We have assumed that only the y-component of the interaction forces are effective and have neglected any net force around the MT circumference.

Relative neighbor dipole coupling forces calculated from eq. (1) and MT geometry are shown in table 1. These relative forces, which we use for transition rules, may be multiplied by 2.3×10^{-14} N to obtain calculated absolute values of inter-subunit forces.

To simulate MT automata, we represent MT structure as a two-dimensional grid in which the cylindrical MT has been filleted open and flattened (figs. 6 and 7). The grid consists of MT subunit dimer loci which can exist in either an α state (blank or blank with dot) or β state (solid black). At each time step (generation), resulting neighbor forces are calculated for each dimer in the grid. The extent to which each dimer is influenced by neighbor forces acting upon its mobile electron is represented by a "threshold" parameter. The higher the threshold, the greater are the summated neighbor forces necessary to induce a transition. For example, a threshold of ± 9.000 means that net neighbor forces greater than $+9.0 \times 2.3 \times 10^{-14}$ N will induce an α state, and negative forces of less than $-9.0 \times 2.3 \times 10^{-14}$ N will induce a β state.

Biological factors which might affect the threshold include temperature, pH, voltage gradients, ionic concentration, genetically determined vari-

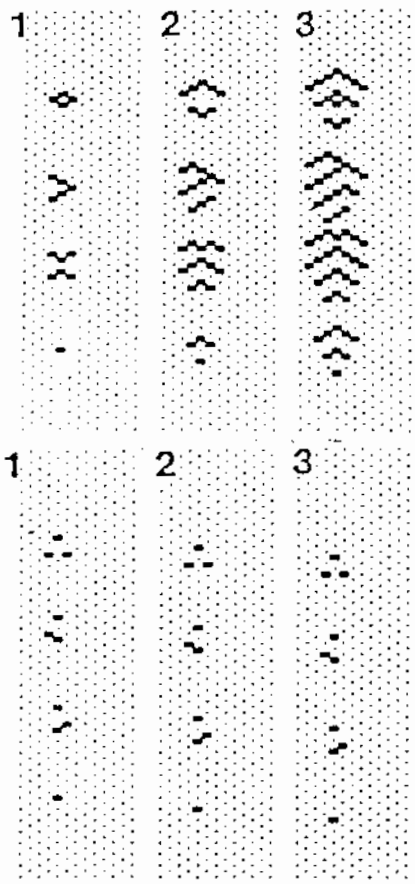

Fig. 6. Some virtual microtubule automata existing for two different threshold values. Top: objects in left panel are labelled (top to bottom) as diamond blinker, triangle glider, spider glider and dot glider. The middle and right sided panels in the top show the next two generations at threshold ±1.000. The objects either blink or move and leave "wakes" which lead to travelling wave structures. Bottom: the first three generations of some other gliders with threshold ±9.000. At this higher threshold, the gliders travel without creating a wake or travelling waves.

ability in individual dimers, and binding of molecules including MAPs and/or drugs to dimer subunits. In nerve cells, travelling membrane depolarizations could induce transient waves of lowered threshold along parallel arrayed MTs. Consequently, the frequency of depolarization for a particular nerve cell would directly influence the elaboration of patterns within that nerve cell's MT automata.

In the MT automata of Smith, Watt, and Hameroff [64] and Hameroff, Smith and Watt [37, 38] boundary conditions were chosen in which reflection of automata patterns occurred at each end of simulated MTs. In more recent studies using toroidal boundary conditions [39], we have investigated effects of varying thresholds on MT automata behavior as well as the effects of asymmetrical thresholds in which α and β transition thresholds differ. The simulations have demonstrated behaviors of both a general nature (e.g. virtual automata, gliders and blinkers) similar to behavior in other automata systems, and of a specific nature (e.g. perturbation stable gliders, wedge patterns, NE–SW orientations) derived from unique MT properties. Threshold-dependent behaviors include gliders (dot, spider, bus and giant gliders), travelling and standing wave patterns, blinkers, linearly growing patterns ("bean sprouts"), bidirectional gliders, and frozen patterns. The bifurcations found in the automata dynamics are summarized in fig. 8.

Having demonstrated the potential capability of MT automata for information processing in single MTs, in the present study we have begun to model simple MT networks as well as MT assembly and disassembly.

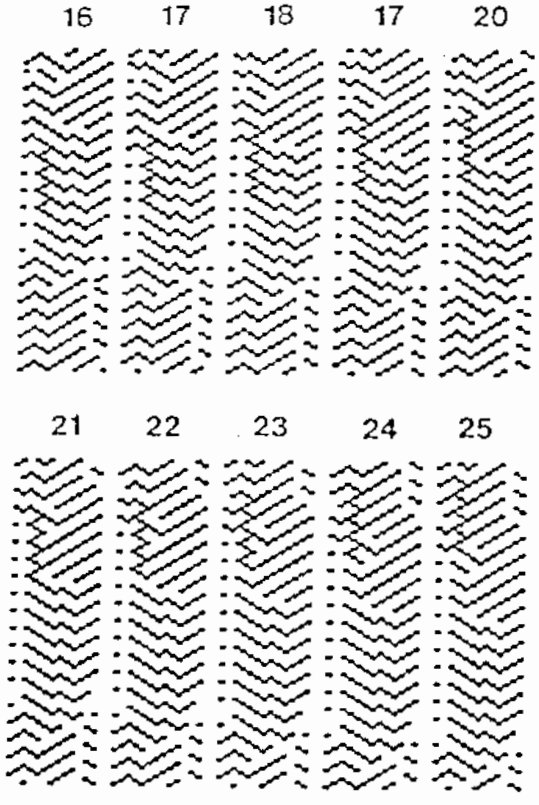

Fig. 7. Time steps 16 through 25 of a microtubule automata simulation with asymmetric threshold, demonstrating localized bilateral information transformation. The initial condition was few randomly scattered α seeds on a β background. The threshold from α to β is −20.000. From β to α the threshold is 2.000. Note that as the β bus (black line of dimers) moves north a new α glider (white line of dimers) is developed in the western region of the neighborhood. This new glider continues to expand until generation 22 when it is "released" from the β bus and starts to travel south together with the other α glider. This dynamical phenomenon may account for the observed bilateral transport on MTs as well as processes related to "back-propagation" in neural networks.

4. A cytoskeletal connectionist network

The largest portion of free energy used in neuronal dendrite cytoplasm is consumed by MAP2, which actively interconnects dendrite MTs and other structures [68]. A number of empirical studies have also shown that cytoskeletal structures within dendrites change during learning. The relation between cognitive structural changes within neurons and among neurons is enigmatic: which is cause and which is effect? In "true" neural networks (i.e. the brain), the formation of new connections, as well as the breakdown of old ones, is presumably a function of both internal neuronal states (configuration and states of the cytoskeleton, membranes, membrane proteins, second messengers, etc.), as well as signals received from other neutrons. Thus, a multi-level hierarchy of information processing is suggested in biological

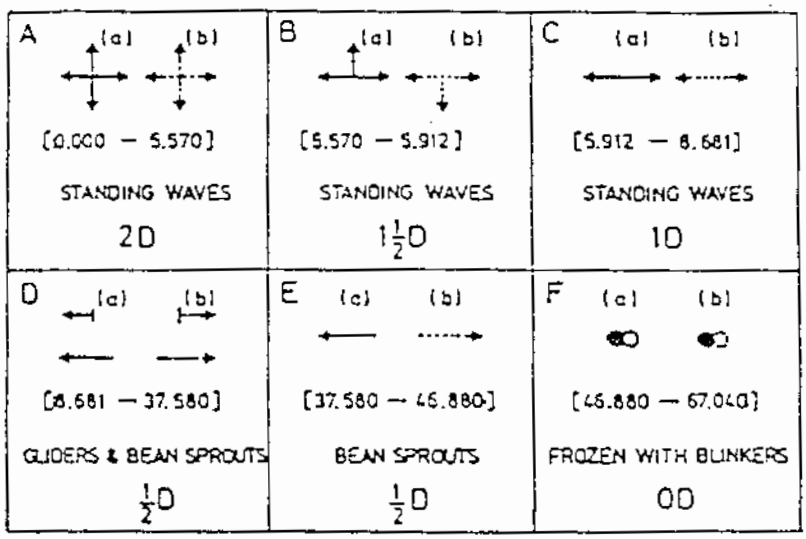

Fig. 8. Bifurcation table for toroidal microtubule automata dynamics with symmetrical dipole coupling thresholds. The upper items in each sector (A)–(F) indicate the dominant global behavior for: (a, solid arrows) β seeds on an α background, and (b, dashed arrows) α seeds induced on a β background. Below the dominant behaviors are the threshold intervals, how we describe each type of dynamic phenomena, and the dimensionality of the growth patterns.

neural networks. To explore this possibility, we have devised an adaptive network based on cytoskeletal structure and function.

Present technologies cannot yet address nanoscale actions of individual protein subunits (although scanning tunnelling microscopy and related techniques may soon be capable). Consequently, there are currently insufficient data to directly test or accurately model such actions and their collective properties.

To merely explore some possibilities, we have used what is known about cytoskeletal structure to serve as the basic architecture for a new connectionist computer. The result is an adaptive dynamical system having certain similarities with the cytoskeleton.

Parallel arrays of MT automata (MTA) are interconnected via MAP-like connections enabling different MTA to communicate with one another. The MAP connections are themselves modeled to be simple automata (MAPA) capable of transmission of signals (sequences of α and β states) from one MTA to another. In the simplest case, this transmission is unidirectional, only transferring signals from a predefined input area on one MTA to a predefined output area on another. Consequently, any tubulin dimer state (α or β) from the MAPA origin on the "input" MTA1 is transmitted to the MAPA target area on the "output" MTA2 (fig. 9).

Conditions which can contribute to dynamic behavior of the MTA network (MTAN) system include MTA thresholds as well as number, attachment locations, and directionality of MAPA. By defining inputs and outputs for each MTA (fig. 10), together with a recursive procedure for updating subunit states, we are able to construct a simple adaptive network.

To model a computationally efficient connectionist network via a feedback between connection topology, internal automata dynamics and automata rules, we use an optimization process often used by Nature: *variation* combined with *selection*. Several systems compete in parallel with respect to a given set of tasks. At each step in the optimization process the most efficient system is selected as the "mother system". At the next step in the optimization process a population of other systems is created as "daughters" or random offspring from the mother system. When one of the offspring begins to perform better than the original system, this offspring is turned into the mother

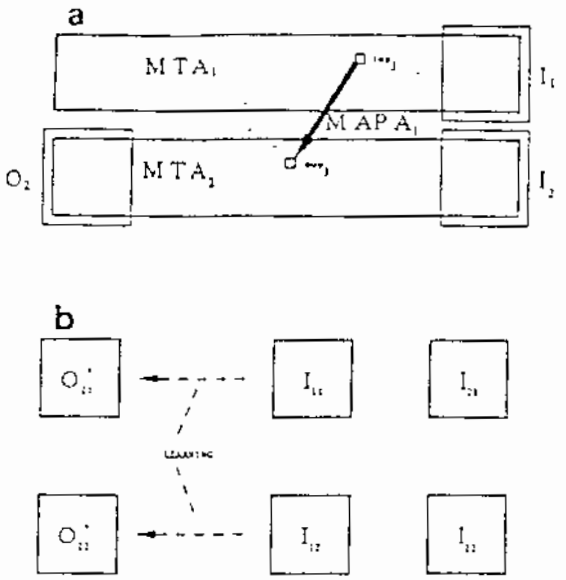

Fig. 9. (a) The simple microtubule automata network, the MTA net, consists of two toroidal MTA of length l dimers, coupled via microtubule associated protein automata, MAPA. The output for the MTA net is defined at the left end of the lower MTA indicated by O_2, and it is taken when the system is updated $l-(13+1)$ times after the input patterns are set at locations I_1 and I_2 at time 0. Input and output areas occupy a matrix area of $13 \times 13 = 169$ dimers. The jth MAPA transmits the dimer states from the input area inp_j at the upper MTA to the output area oup_j at the lower MTA. For each pair of input patterns, I_1 and I_2 at the upper and lower MTA, there exists a desired output pattern O_2^* at the lower MTA. (b) By means of the learning algorithm, the mappings $(I_{11}, I_{21}) \rightarrow O_{21}^*$ and $(I_{12}, I_{22}) \rightarrow O_{22}^*$ are generated.

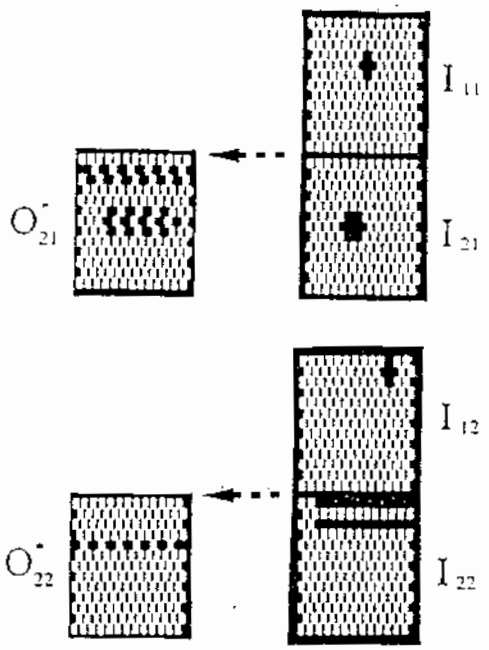

Fig. 10. A MTA network with start configurations (I_{11}, I_{21}) and (I_{12}, I_{22}) and corresponding desired output patterns O_{21}^* and O_{22}^*. These two maps have been chosen from the learnable set for the MTA network. The structure of this set is as yet unknown. The present realization of the MTA network is not able to satisfy every input–output pattern combination.

system as the next step in the optimization process. In this way it is possible to evolve efficient networks with respect to different computational tasks.

In our initial efforts to model a cytoskeletal network, two parallel MTA are capable of being interconnected by MAPA at any subunit loci. Each MTA has an input area at the right end, and output area at the left. Output area states are compared to desired output states using their Hamming distance. For the system to recognize inputs to produce desired outputs, we have random MAPA connections between the two MTA. The learning algorithm for our network is represented both by the threshold parameter for the individual MTA and by the interconnections between the different MTA. A detailed description of the learning algorithm is given in the appendix.

The MTAN obtains truly distributed computation since it is only governed by low-level, neighborhood interactions mediated by intermolecular forces. Such a spatial locality is usually not found in other connectionist models. Another important difference is that the learning algorithm for the MTAN does not use a local learning rule as most artificial neural networks do; rather, MTAN uses an *evolutionary search* to accomplish learning. However, our current MTAN system needs input/output learning in the same sense as most artificial neural net systems do.

In the following example we have fixed the threshold parameters for the upper and the lower MTA at ± 5.900 and ± 9.000 respectively. The corresponding input–output maps used for learning are shown in fig. 10. The connection topology

$C_j = C_2$ for the first accepted input–output map is shown in fig. 11 together with the dynamics for the MTA net at time 0, 43, and 66. The Hamming distance between the desired and the actual map is $H_d = 0$. In fig. 12 the connection topology $C_k = C_4$ for the second input–output map is shown together with the dynamics at time 0, 23, and 66 ($H_d = 0$). It turns out that C_4 also satisfies the first input–output map. We had to redo pass (5) and (6) in the learning algorithm a number of times before the system found a correct C_k satisfying both the maps $(I_{11}, I_{21}) \rightarrow O_{21}^*$ and $(I_{12}, I_{22}) \rightarrow O_{22}^*$.

In the situations where the two pattern combinations can be memorized, there always seem to be several C_k's satisfying the two maps. However, the present realization of the network is not able to memorize every pattern combination at the same time. Some maps cannot coexist.

The MTA net is also able to "associate" or generalize patterns. In figs. 13a and 13b the system tries to associate or recognize the first input pattern, and in 13c and 13d the system tries to associate the second pattern. Note that H_d may be quite high due to a simple horizontal offset, even though the patterns seem very similar. The basis for this associative ability is the existence of relatively perturbation-stable virtual automata in this system. The dynamics of the system is more

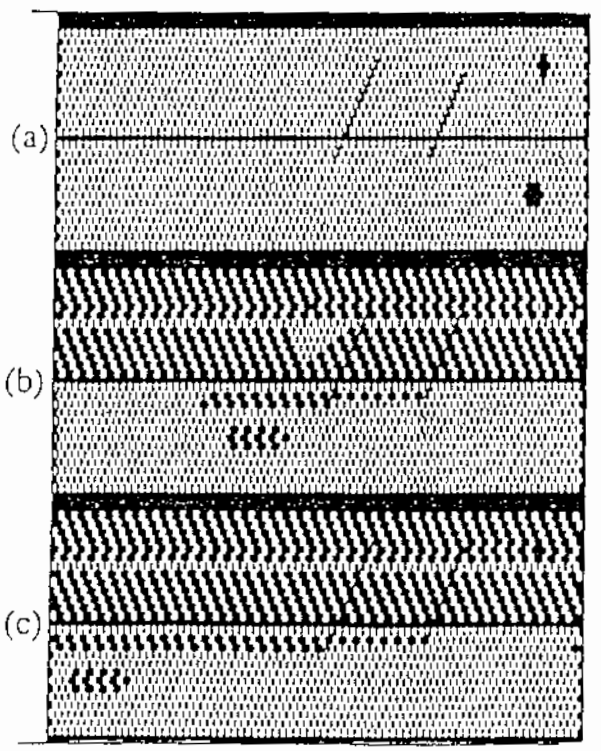

Fig. 11. MTA net at stage (3) in the learning process. The parameters for this net are $I = 80$ and $\text{inp}_j = \text{oup}_j = 1$. The connection topology $C_j = C_2$, with MAPA at the dimer locations $(60,6) \rightarrow (55,2)$ and $(47,4) \rightarrow (41,3)$, turns out to satisfy the first input–output map. The Hamming distance $H_d = |O_{21}^* - O_{21}| = 0$. The dynamics is shown at time: (a) 0, (b) 43, and (c) 66. The thresholds for the upper and lower MTA are ± 5.900 and ± 9.000 respectively.

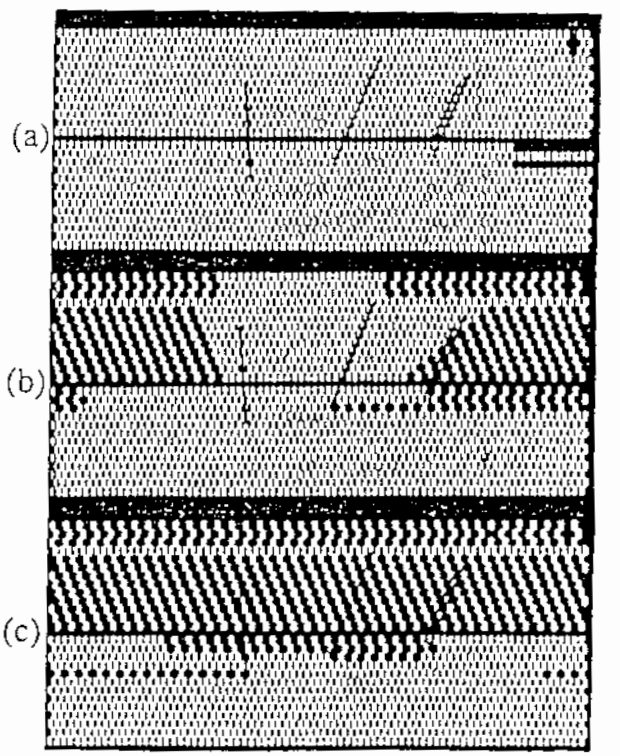

Fig. 12. The same MTA net as shown in fig. 11 at stage (5) in the learning process. $C_k = C_4$ is here given by: $(60,6) \rightarrow (55,2)$, $(47,4) \rightarrow (41,3)$, $(59,7) \rightarrow (55,1)$, and $(28,7) \rightarrow (29,5)$. The dynamics is shown at time: (a) 0, (b) 26, and (c) 66. It can be shown that C_4 both satisfies the first and the second input–output map ($H_d = 0$). However, pass (5) and (6) had to be repeated a number of times, with $D = 10$, before a correct connection topology was found. The thresholds for the upper and lower MTA are still ± 5.900 and ± 9.000 respectively.

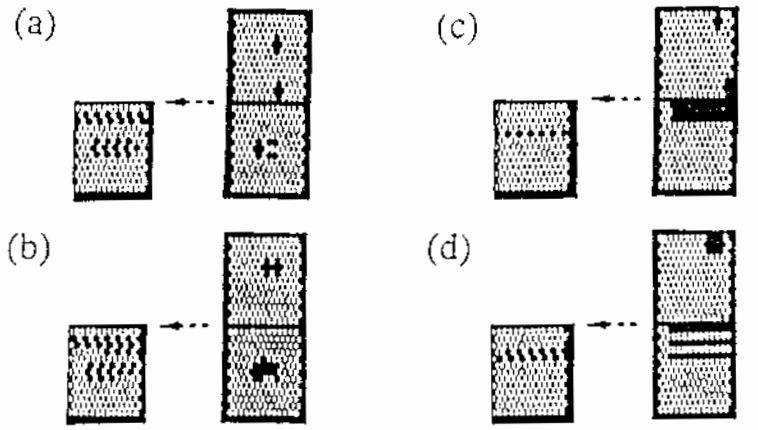

Fig. 13. Association of patterns in the MTA net with connection topology C_4. (a) and (b) are related to the first map, and (c) and (d) are related to the second map. In (a) $H_d = 26$ and in (b) $H_d = 6$ although (a) looks more right than (b). (c) is perfectly associated. In (d) we see a less correctly associated pattern, $H_d = 26$. Compare with fig. 10.

resistant to perturbations in the longitudinal (north–south) MTA direction than in the east–west direction. This property appears due to chosen threshold values which mainly support communication along the north–south axis on the MTA (see the bifurcation table in fig. 8). The reason for the preferred north–south communication for higher thresholds is due to the geometry of the MT lattice. The east–west interactions between most of the dipole configurations are simply cut off for higher thresholds. For example, table 1 shows relative forces for the 24 configuration pairs occurring. None of the pairwise east–west interactions exceed an absolute value of the relative force larger than $15.205 \times 2.3 \times 10^{-14}$ N. The pairwise north–south interactions have absolute values up to $62.500 \times 2.3 \times 10^{-14}$ N.

Selection of specific asymmetric threshold values which differ between the two connected MTA as well as selection of different background states in the two connected MTA can lead to significant behavior. For example, a larger absolute positive threshold in MTA1 and a larger absolute negative threshold in MTA2 cause north → south direction gliders in MTA1 which induce, by MAPA connections, south → north gliders in MTA2. Another example of retrograde information transport is a system with MAPA connections between MTA in different ground states. This is possible since β-gliders always travel south on an α background and α-gliders always travel north on a β background (for details on the dynamics in a single MTA, see ref. [39]). Such retrograde signaling could implement "back-propagation" within neural net neurons. MTs from separate dendritic branches merge and interconnect in the dendrite; thus dendritic MTA nets can merge information from multiple dendritic branch synapses. "Up-regulation" due to increased activity in one synaptic area could thereby "down-regulate" relatively inactive synapses on separate dendritic branches.

Although our system presently is able to adapt to certain dynamics, the learning process is not optimal for several reasons. These include the basis on which the daughter systems are both constructed and chosen, and because of an inefficient use of the MTA patterns. Also, the Hamming distance is probably not the best index for selection of a connection topology because two identical patterns shifted just for one dimer often result in a huge Hamming distance. This behavior also limits the associative properties.

Several potential improvements could be implemented in the MTA net system. The resolution of

different maps on the same MTA net would increase significantly if the system were able to use "coded" MAPA. A coded MAPA could be an automaton which only transmits if a certain α/β sequence ("an initiator pattern") passes the input area for the MAPA. Similarly, the MAPA should stop the transmission whenever a certain stop pattern passes the input area; thus the system would have properties very similar to the DNA transcription system. Alternatively, the MAPA could be coded to transmit a signal averaged over a certain area in the input zone. Another possible improvement which could reflect true biological activity involves MAPA connection patterns. Rather than random connection topologies, MTA patterns could determine where the MAPA connections should be located. For example, connection sites could be determined by the location of a persistent diamond blinker or some other pattern occupying roughly $2 \times 2 = 4$ dimer subunits. These possibilities have yet not been tested, but indicate a potential for adaptation and learning in structures based on cytoskeletal networks. Future work will explore these areas.

Assembly and disassembly of MTs, MAPs, centrioles and other cytoskeletal structures determine cell division, differentiation, movement, transport, and (in neurons) synaptic connectivity. Coupling between MTA dynamics and MT assembly/disassembly could explain the orchestration of these elegant and delicate functions. In section 5, we investigate this area.

5. Assembly and disassembly of microtubules

Experimental results of studies on assembly and disassembly of MTs both in vivo and in vitro are summarized in ref. [11]. In order to grow, the microtubule must have dimers containing exchangable GTP at the end. Without this GTP "cap", depolymerization occurs unless the MT is stabilized by other factors such as binding to other cytoskeletal structures. Thus, free MTs tend to either grow or shrink. These results support the dynamic instability model of MT assembly and disassembly [45]. In a simple cellular automaton model for such a process, each boundary site can be considered to be in one of five different states: as polymerized tubulin dimers with either GTP or GDP, as free tubulin with either GTP or GDP, or as water. The possible transitions are shown in fig. 14.

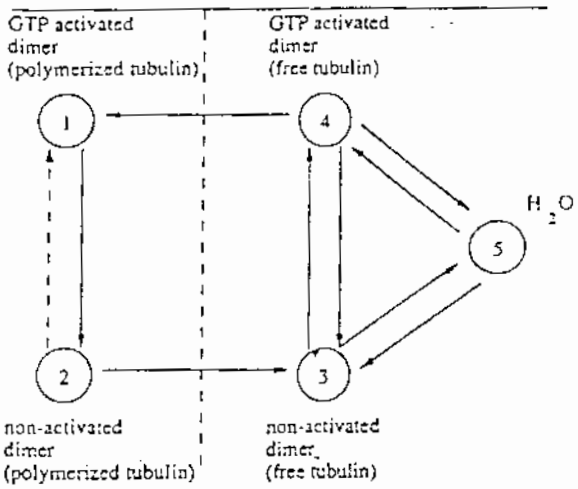

Fig. 14. State diagram for a simple model of assembly/disassembly of microtubules. State 1 is GTP activated tubulin dimer in polymerized form (microtubule geometry), state 2 is microtubule tubulin is non-activated form (GDP), state 3 is non-activated free dimer (in solution), state 4 is GTP activated free dimer, and state 5 is water. The transitions are discussed in the text. Note that this model is formulated partly as a Markov chain, and partly as a cellular automaton.

In the present study, we are concerned with the elongation of already existing tubules, since formation of initial fragments is governed by complex nucleation processes and interactions with centrioles.

We assume that the GTP hydrolysis to form GDP tubulin occurs through a process $(1 \rightarrow 2)$ described by some probability P_{12} at each update of the system (fig. 14). The disassembly $(2 \rightarrow 3)$ of the MTs occurs through dissolving of the non-activated dimers. This process is assumed to depend on the concentration of activated free tubulin [11]: a polymerized boundary dimer will

get free if a major part (three or more) of its neighbors is of the non-GTP free form (including water). Thus, the lower the GTP-activated free dimer concentration, the faster the disassembly. In this model both the concentration of the activated GTP tubulin and the non-activated GDP tubulin are determined by a stochastic process involving internal transitions between the three states: 3, 4, and 5. The higher the overall probability for the presence of an activated dimer among the free states, the more likely is a polymerization process in the system. Polymerization ($4 \rightarrow 1$) takes place if an activated free dimer is aligned with at least two activated polymerized dimers. A necessary condition for polymerization is that the fractional occupation time for activated dimer among the free states is significantly higher than the decay probability P_{12} for the activated microtubule dimer. The transition $2 \rightarrow 1$ is not modeled at this point, but will be discussed later.

Simulations of microtubule assembly and disassembly with the simple model are shown in fig. 15. The clocking frequency in this model is significantly lower than the assumed clocking frequency for signal propagation on the microtubule (10^9–10^{11} Hz). Elongation of existing dentrite MTs in vivo may result in a MT growth of 1 mm/day corresponding to 1 nm/s (or one dimer row per 8 s), although in vitro assembly under physiological conditions may elongate at least two orders of magnitude faster. The simulation in figs. 15d–15f shows an elongation rate of approximately 6 times 8 nm for each 50 generations. This corresponds to approximately 1 nm/s. Therefore the updating of the assembly/disassembly model does not demand nearly the same frequency as the signal propagation model does (10^9–10^{11} Hz). In the present simulation we update with a real time of only 1 Hz.

If specific dynamics on the MTA are able to activate dimers at certain locations, for instance at the free ends (the $2 \rightarrow 1$ transition), there exists an internal mechanism for determining whether a microtubule in the network should start growing. Introducing to the simple cytoskeletal model from

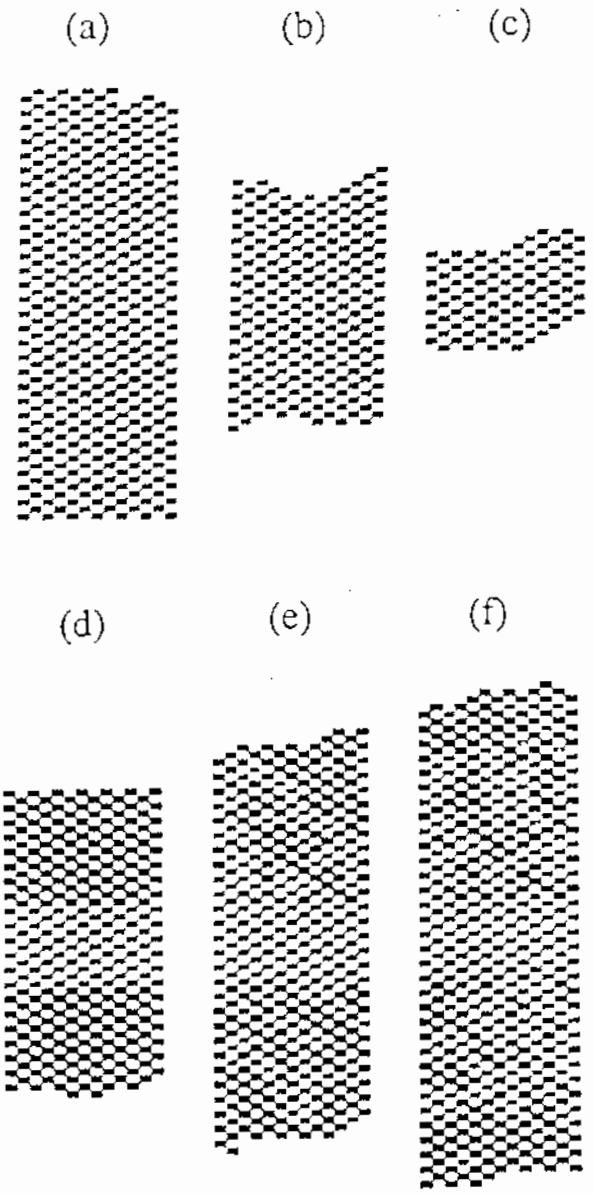

Fig. 15. (a)–(c) disassembly of a microtubule shown at time 0, 21, and 49, with hydrolysis probability $P_{12} = 0.05$ per generation, and an overall probability of 0.091 that the free states are visited by an activated dimer during the automaton generation time. Non-activated microtubule tubulin dimers (state 2) are represented by shaded squares, whereas the free tubulin and water are blank (states 3, 4, and 5). (d)–(f) Assembly of a microtubule with GTP activated caps (state 1 shown as dark squares), shown at time 0, 20, and 50, with hydrolysis $P_{12} = 0.05$ per generation, and an overall probability of 0.987 that the free states are visited by an activated dimer during the automaton generation time.

section 4, such a mechanism adds another feedback between local dynamics and meta-dynamics of our network. Relevant to section 4, selecting the sites of MAPA connections by means of MTA dynamics would also be consistent with this type of feedback.

In vivo assembly/disassembly of MTs may actually be controlled by signals transmitted on the cytoskeleton.

6. Discussion: connectionism in the cytoskeleton

Deciphering of the genetic code in DNA and RNA has led to many technological applications. The existence of a "real-time" processing code in the cytoskeleton could be comparably useful because of the important functions which could be controlled or regulated (mitosis, differentiation, aging, growth, immune function, etc.).

In the neuronal cytoskeleton, MTA can be relevant to brain/mind cognitive function. For example, MT automata may be utilized for guidance and movement of cells and cell processes (axon growth cones, dendritic spines) during morphogenesis of the brain's network architecture. In learning, axoplasmic transport and other mechanisms orchestrated by MT automata could regulate synaptic plasticity. Threshold-dependent bidirectional MT automata patterns indicate that a "back-propagation" type of synaptic regulation could occur because rapid information transport in directions opposite to the nerve impulse is possible. Combined with possible retrograde information flow across synapses ("trophism", pre-synaptic modulation) the cytoskeleton could support "neural-net" type phenomena in the brain. Beyond these morphological roles, MT automata could themselves directly participate an imprinting, pattern recognition, memory and other cognitive functions. MT automaton gliders (8 to 800 m/s) may exist as traveling waves, coupled to nerve membrane depolarizations. Coupling between membrane events and MT automaton behaviors may occur via ionic fluxes or direct connection through specialized sub-membrane cytoskeletal proteins such as ankyrin, fodrin and spectrin to the cytoskeleton. This coupling can lead to a view of the brain as a hierarchy of networks with a cytoskeletal basement level. MT automata would then comprise the "fine grain" of cognition, the "roots of consciousness".

Relegating cognition function to the level of protein conformational dynamics is supported by efforts to understand the mechanism of general anesthesia. Anesthetic gas molecules erase consciousness (while sparing other brain functions like breathing) by inhibiting conformational switching in classes of proteins such as receptors, ion channels, enzymes and cytoskeletal subunits [25]. The anesthetic molecules are thought to bind in hydrophobic regions within these proteins: the same sites proposed by Fröhlich to house dipole oscillations. Anesthetics such as halothane have also been shown (at relatively high concentrations) to cause depolymerization of microtubules [1]. Anesthesia (the reversible cessation of consciousness) may be due to interruption of communicative interactions within and among cytoskeletal networks and their membrane connections.

We have demonstrated that a population of simple networks of paired MTA is able to learn two different patterns by using an evolutionary mechanism as well as associate nearby patterns. However, many improvements may be implemented in the model which can (a) more closely resemble biological activities, and (b) increase MTA network performance. Some of these are discussed in section 4.

We have described the cytoskeleton as a connectionist information network. As such, it may be compared with other connectionist systems like artificial neural networks, classifier systems, etc. Farmer (these Proceedings [23]) has described a group of parameters into which all such systems may be fit for comparison and clarity. These parameters include nodes, states, connections, parameters, interaction rules, learning algorithm and metadynamics. In table 2, we have catalogued

Table 2
Farmer's Rosetta Stone [23] for adaptive dynamic systems applied to microtubule automata (MTA).

	Single MT	MTA networks
nodes	cellular automata cells; MTA subunits	cellular automata networks; MTA-MAPA
states	α and β state patterns	α and β state patterns
connections	lattice geometry	MAPA and other connections
parameters	local thresholds	coding in MAPA connections
interaction rules	local dipole coupling forces	MAPA connections
learning algorithm	input/output learning; selection of the best in a population (selectionist learning)	input/output learning; selection of the best in a population (selectionist learning)
metadynamics	local threshold changes; metastable states	threshold change in MTA-MAPA loci and assembly/disassembly

both a single MT automaton and the adaptive MT automaton network according to Farmer's connectionist classifications.

Connectionist networks within single elements of larger connectionist networks suggest a self-similar "fractal-like" relationship. Information capacity of a high-resolution scale within a self-similar structure is far greater than the capacity at larger scales. Roboticist Hans Moravec [56] has attempted to compare the computing power of a computer and of the human brain. Considering the number of next states available per time in binary digits, a microcomputer has a capacity of about 10^6 bits per second. Moravec calculates brain "computing" power by assuming 40 billion neurons, each with perhaps one thousand synaptic connections which can change states hundreds of times per second, resulting in 4×10^{15} bits per second. We estimate approximately 10^{14} MT tubulin subunits in a human brain based on MTs spaced 100 nm apart and 40% of brain volume being neuronal cytoplasm. In our model of MT automata these 10^{14} brain MT subunits can change states 10^9 to 10^{11} times per second leading to a total brain capacity of 10^{23} to 10^{25} bits per second! Such a huge capacity could provide a high resolution to the grain of cognition, permit massive parallelism and redundancy, and account for cytoplasmic "housekeeping" chores not directly related to brain/mind function. Still, is such a huge capacity necessary to explain cognitive function? That question is presently unanswerable. However, we surmise that the highest level of brain/mind cognitive functions are collective emergent effects whose fine grain may exist within the cytoskeleton.

We conclude with possible applications of MTA molecular cognition. Deciphering real-time MTA codes may permit interfacing to emerging technologies such as spinoffs of scanning tunneling microscopy. These techniques should allow nanometer scale monitoring and programming of dynamic actions of individual protein subunits within assemblies such as MTs. Combining ge-

netic engineering of MT tubulin subunits with real-time programming could lead to replicating MTA with complex, purposeful activities. Perhaps akin to programmable viruses, mobile MTA might be capable of intracellular repair with profound medical applications.

Acknowledgements

We appreciate the discussions we had with Kuni Kaneko on how to design the input and the output for the adaptive microtubular automaton network.

Appendix. The learning algorithm

The process of teaching the MTA net to map two different sets of input to two different output patterns consists of six steps.

(1) Primarily depending on the shape of the desired output pattern, the thresholds for both MTA are set manually. This step demands certain knowledge about what kind of dynamics is possible for each value of the threshold parameter (recall fig. 8), and is not yet endogenous in the algorithm.

(2) A single random MAPA connection is placed at D successive MTA nets. Each of these MTA nets are then simulated for $I-(13+1)$ generations, at which time the Hamming distance, H_d, between the actual output O_{21}, and the desired output pattern, O_{21}^*, is calculated. The MAPA connection pattern which resulted in the smallest H_d with the two first input patterns (I_{11}, I_{21}) is kept for the next steps. This new connection topology is denoted by C_1.

(3) With C_1 as the basic (mother) system, D new random MAPA connections are tested in D different (daughter) systems. Again the system with the smallest $H_d = |O_{21}^* - O_{21}|$ is chosen. This new connection topology is denoted by C_2. (3) is then repeated until an acceptable H_d is reached. The connection topology for the new system is denoted by C_j.

(4) I_{11} and I_{21} are now replaced with I_{12} and I_{22}, still conserving C_j.

(5) Additional MAPA to C_j as in step (3) which is repeated until an acceptable $H_d = |O_{22}^* - O_{22}|$ is reached for a new C_k.

(6) The map $(I_{11}, I_{21}) \rightarrow O_{21}^*$ is then tested with C_k. If $|O_{21}^* - O_{21}|$ still is acceptable, the sequence is finished satisfactorily. If not, the sequence is either started all over again at (1) or repeated from (5).

References

[1] A.C. Allison and J.F. Nunn, Effects of general anaesthetics on microtubules. A possible mechanism of anaesthesia, Lancet 2 (1968) 1326–1329.

[2] J. Alvarez and B.J. Ramirez, Axonal microtubules: their regulation by the electrical activity of the nerve, Neurosci. Lett. 15 (1979) 19–22.

[3] D.J. Amit, Modeling Brain Function, The World of Attractor Neural Networks (Cambridge Univ. Press, Cambridge, 1989).

[4] L.A. Amos and A. Klug, Arrangement of subunits in flagellar microtubules, J. Cell Sci. 14 (1974) 523–550.

[5] C. Aoki and P. Siekevitz, Plasticity in brain development, Sci. Am. (December 1988) 34–42.

[6] J. Atema, Microtubule theory of sensory transduction, J. Theor. Biol. 38 (1973) 181–190.

[7] H. Athenstaedt, Pyroelectric and piezoelectric properties of vertebrates, Ann. NY Acad. Sci. 238 (1974) 68–93.

[8] R. Audenaert, L. Heremans, K. Heremans and Y. Engleborghs, Secondary structure analysis of tubulin and microtubules with Raman spectroscopy, Biochim. Biophys. Acta 996 (1989) 110–115.

[9] M.P. Barnett, Molecular systems to process analog and digital data associatively, in: Proceedings of the 3rd Molecular Electronic Device Conference, ed. Forrest Carter, Naval Research Laboratory, Washington, DC, 1987.

[10] J.S. Becker, J.M. Oliver and R.D. Berlin, Fluorescence techniques for following interactions of microtubule subunits and membranes, Nature 254 (1975) 152–154.

[11] A.D. Bershadsky and J.M. Vasiliev, Cytoskeleton, in: Cellular Organelles, ed. P. Siekevitz (Plenum Press, New York, 1988).

[12] R.B. Burns, Spatial organization of the microtubule associated proteins of reassembled brain microtubules, J. Ultrastruct. Res. 65 (1978) 73–82.

[13] P.S. Churchland and T.J. Sejnowski, Perspectives on cognitive neuroscience, Science 242 (1988) 741–745.

[14] M. Conrad, On design principles for a molecular computer, Commun. ACM 28 (1985) 464–480.

[15] M. Conrad, W. Guttinger and M. Dal Cin, Lecture Notes in Biomathematics, Vol. 4. Physics and Mathematics of the Nervous System, Proceedings of a Summer School Organized by the International Centre for Theoretical Physics, Trieste, and the Institute for Information Sciences, University of Tubingen, 1973.

[16] J. Cronly-Dillon, D. Carden and C. Birks, The possible involvement of brain microtubules in memory fixation, J. Exp. Biol. 61 (1974) 443–454.

[17] M. De Brabander, A model for the microtubule organizing activity of the centrosomes and kinetochores in mammalian cells, Cell Biol. Intern. Rep. 6 (1982) 901–915.

[18] M. De Brabander and J. DeMey, eds., Microtubules and Microtubule Inhibitors, Proceedings of the 3rd International Symposium, Beerse, Belgium, 3–6 September 1985 (Elsevier, Amsterdam, 1985).

[19] M. De Brabander, G. Geuens, J. DeMey and M. Joniav, The organized assembly and function of the microtubule system throughout the cell cycle, in: Cell Movement and Neoplasia, ed. M. De Brabander (Pergamon Press, Oxford, 1986).

[20] A.M. De Callataÿ, Natural and Artificial Intelligence. Processor Systems Compared to the Human Brain (North-Holland, Amsterdam, 1986).

[21] N.L. Desmond and W.B. Levy, Anatomy of associative long-term synaptic modification, in: Long-Term Potentiation: From Biophysics to Behavior, eds. P.W. Landfield and S.A. Deadwyler (1988).

[22] P. Dustin, Microtubules, 2nd revised Ed. (Springer, Berlin, 1984) p. 442.

[23] D. Farmer, A Rosetta Stone for connectionism, Physica D 42 (1990) 153–187, these Proceedings.

[24] S.R. Farmer, G.S. Robinson, D. Mbangkollo, J.F. Bond, G.B. Knight, M.J. Fenton and E.M. Berkowitz, Differential expression of the B-tubulin multigene family during rat brain development, Ann. NY Acad. Sci. 466 (1986) 41–50.

[25] N.P. Franks and W.R. Lieb, Molecular mechanisms of general anesthesia, Nature 300 (1982) 487–493.

[26] W.J. Freeman, Mass Action in the Nervous System (Academic Press, New York, 1975).

[27] H. Fröhlich, Long range coherence and the actions of enzymes, Nature 228 (1970) 1093.

[28] H. Fröhlich, The extraordinary dielectric properties of biological materials and the action of enzymes, Proc. Natl. Acad. Sci. 72 (1975) 4211–4215.

[29] H. Fröhlich, Coherent excitations in active biological systems, in: Modern Bioelectrochemistry, eds. F. Gutmann and H. Keyzer (Plenum Press, New York, 1986) pp. 241–261.

[30] M.S. Gazzaniga, The Social Brain – Discovering the Networks of the Mind (Basic Books, New York, 1985).

[31] I. Ginzburg, A. Teichman and V.Z. LiHaver, Isolation and characterization of two rat alpha-tubulin isotopes, Ann. NY Acad. Sci. 466 (1986) 31–40.

[32] S. Grossberg, ed., The Adaptive Brain I. Cognition, Learning, Reinforcement and Rhythm (North-Holland, Amsterdam, 1987).

[33] W. Grundler and F. Keilmann, Sharp resonances in yeast growth prove nonthermal sensitivity to microwaves, Phys. Rev. Lett. 51 (1983) 1214–1216.

[34] F. Gutmann, Some aspects of charge transfer in biological systems, in: Modern Bioelectrochemistry, eds. F. Gutmann and H. Keyzer (Plenum Press, New York, 1986) pp. 177–197.

[35] S.R. Hameroff, Ultimate Computing: Biomolecular Consciousness and Nanotechnology (North-Holland, Amsterdam, 1987).

[36] S.R. Hameroff and R.C. Watt, Information processing in microtubules, J. Theor. Biol. 98 (1982) 549–561.

[37] S.R. Hameroff, S.A. Smith and R.C. Watt, Nonlinear electrodynamics in cytoskeletal protein lattices, in: Nonlinear Electrodynamics in Biological Systems, eds. W.R. Adey and A.F. Lawrence (Plenum Press, New York, 1984) pp. 567–583.

[38] S.R. Hameroff, S.A. Smith and R.C. Watt, Automaton model of dynamic organization in microtubules, Ann. NY Acad. Sci. 466 (1986) 949–952.

[39] S.R. Hameroff, S. Rasmussen and B. Mansson, Molecular automata in microtubules: basic computational logic for the living state?, in: Artificial Life, the Santa Fe Institute Studies in the Sciences of Complexity, Vol. VI, ed. C. Langton (Addison–Wesley, Reading, MA, 1989) pp. 521–553.

[40] D.O. Hebb, The Organization of Behavior (Wiley, New York, 1949).

[41] J.J. Hopfield, Neural networks and physical systems with emergent collective computational abilities, Proc. Natl. Acad. Sci. 79 (1982) 2554–2558.

[42] J. Jaynes, The Origin of Consciousness and the Breakdown of the Bicameral Mind (Alan Payne, Penguin Books, London, 1976).

[43] M. Karplus and J.A. McCammon, Protein ion channels, gates, receptors, in: Dynamics of Proteins: Elements and Function, Ann. Rev. Biochem., ed. J. King (Benjamin/Cummings, Menlo Park, 1983) pp. 263–300.

[44] M. Karplus and J.A. McCammon, Protein structural fluctuations during a period of 100 ps, Nature 277 (1979) 578.

[45] M. Kirschner and T. Mitchison, Beyond self assembly: from microtubules to morphogenesis, Cell 45 (1986) 329–342.

[46] T. Kobayashi, S. Tsukita, S. Tsukita, Y. Yamamoto and G. Matsumoto, Subaxolemmal cytoskeleton in squid giant axon, I. Biochemical analysis of microtubules, microfilaments, and their associate high-molecular-weight proteins, J. Cell. Biol. 102 (1986) 1699–1709.

[47] C.G. Langton, Computation at the edge of chaos, Physica D 42 (1990) 12–37, these Proceedings.

[48] R.J. Lasek, The dynamic ordering of neuronal cytoskeletons, Neurosci. Res. Prog. Bull. 19 (1981) 7–31.

[49] J.C. Lee, D.J. Field, H.J. George and J. Head, Biochemical and chemical properties of tubulin subspecies, Ann. NY Acad. Sci. 466 (1986) 111–128.

[50] M.R. Lindeburg, Engineer in training review manual professional publications, San Carlos, CA (1982).
[51] G. Lynch and M. Baudry, Brain spectrin, calpain and long-term changes in synaptic efficacy, Brain. Res. Bull. 18 (1987) 809–815.
[52] S. Mascarenhas, The electret effect in bone and biopolymers and the bound water problem, Ann. NY Acad. Sci. 238 (1974) 36–52.
[53] G. Matsumoto and H. Sakai, Microtubules inside the plasma membrane of squid giant axons and their possible physiological function, J. Membr. Biol. 50 (1979) 1–14.
[54] R. Mileusnic, S.P. Rose and P. Tillson, Passive avoidance learning results in region specific changes in concentration of, and incorporation into, colchicine binding proteins in the chick forebrain, Neur. Chem. 34 (1980) 1007–1015.
[55] M. Minsky, The Society of Mind (Simon and Schuster, New York, 1986).
[56] H. Moravec, Mind Children (University Press, San Francisco, 1987).
[57] S. Ochs, Axoplasmic Transport and Its Relation to Other Nerve Functions (Wiley–Interscience, New York, 1982).
[58] N. Packard, Adaption towards the edge of chaos, preprint (1988).
[59] K.H. Pribram, Languages of the Brain: Experimental Paradoxes and Principles (Brandon House, New York, 1971).
[60] B. Pullman and A. Pullman, Electronic delocalization and biochemical evolution, Nature 196 (1983) 1127–1142.
[61] G.R. Reeke and G.M. Edelman, Selective networks and recognition automata, in: Computer Culture: The Scientific, Intellectual, and Social Impact of the Computer, ed. H.R. Pagels, Ann. NY Acad. Sci. 426 (1984) 181–201.
[62] L.E. Roth and D.J. Pihlaja, Gradionation: hypothesis for positioning and patterning, J. Protozoology 24 (1977) 2–9.
[63] A.C. Scott, Neurophysics (Wiley, New York, 1977).
[64] S.A. Smith, R.C. Watt and S.R. Hameroff, Cellular automata in cytoskeletal lattices, Physica D 10 (1984) 168–174.
[65] D. Soifer, Factors regulating the presence of microtubules in cells, in: Dynamic Aspects of Microtubule Biology, ed. D. Soifer, Ann. NY. Acad. Sci. 466 (1986) 1–7.
[66] G.C. Somjen, Neurophysiology, The Essentials (Williams and Wilkins, Baltimore, 1983).
[67] H. Stebbings and C. Hunt, The nature of the clear zone around microtubules, Cell Tissues Res. 227 (1982) 609–617.
[68] W.E. Theurkauf and R.B Vallee, Extensive cAMP-dependent and cAMP-independent phosphorylation of microtubule associated protein 2, J. Biol. Chem. 258 (1983) 7883–7886.
[69] S.N. Timasheff, R. Melki, M.F. Carlier and D. Pantaloni, The geometric control of tubulin assemblies: cold depolymerization of microtubules into double rings, J. Cell Biol. 107 (1988) 243a.
[70] S. Tsukita, S. Tsukita, T. Kobayashi and G. Matsumoto, Subaxolemmal cytoskeleton in squid giant axon, II. Morphological identification of microtubules and microfilament-associate domains of axolemma, J. Cell Biol. 102 (1986) 1710–1725.
[71] P. Vassilev, M. Kanazirska and H.T. Tien, Intermembrane linkage mediated by tubulin, Biochem. Biophys. Res. Comm. 126 (1985) 559–565.